Published in final edited form as:
Science. 2010 August 20; 329(5994): 956–959. doi:10.1126/science.1189072.

Linear Arrays of Nuclear Envelope Proteins Harness Retrograde Actin Flow for Nuclear Movement

G.W. Gant Luxton[1,*], **Edgar R. Gomes**[1,2,3,*], **Eric S. Folker**[1], **Erin Vintinner**[1], and **Gregg G. Gundersen**[1,4]

[1]Department of Pathology and Cell Biology, Columbia University, New York, NY 10032, USA

[2]UMR S 787 INSERM, Université Pierre et Marie Curie Paris VI, Paris, 75634, France

[3]Groupe Hospitalier Pitié-Salpêtrière, Institut de Myologie, Paris, 75013, France

Abstract

Nuclei move to specific locations to polarize migrating and differentiating cells. Many nuclear movements are microtubule-dependent. However, nuclear movement to reorient the centrosome in migrating fibroblasts occurs through an unknown actin-dependent mechanism. Here, we found that linear arrays of outer (nesprin2G) and inner (SUN2) nuclear membrane proteins assembled on and moved with retrogradely moving dorsal actin cables during nuclear movement in polarizing fibroblasts. Inhibition of nesprin2G, SUN2 or actin prevented nuclear movement and centrosome reorientation. The coupling of actin cables to the nuclear membrane for nuclear movement via specific membrane proteins indicates that like plasma membrane integrins, nuclear membrane proteins assemble into actin-dependent arrays for force transduction.

Directed nuclear movements are important for establishing cellular polarity during cell migration, development, homeostasis, and ensuring the equal distribution of genetic material during cell division (1–3). Most nuclear movements are microtubule-mediated; however, growing numbers of actin-dependent nuclear movements have been recognized (1, 2, 4–10). Mechanisms for actin-dependent nuclear movement are unclear.

In NIH3T3 fibroblasts polarizing for migration into in vitro wounds, an actin-dependent nuclear movement is triggered by serum or the serum factor lysophosphatidic acid (LPA) and this reorients the centrosome toward the leading edge (5). Nuclear movement and actin retrograde flow occur at the same rate, but how actin is coupled to the nucleus is unknown. We explored the possible involvement of the LINC (linker of nucleoskeleton and cytoskeleton) complex, which spans the inner and outer nuclear membranes (INM and ONM, respectively). LINC complexes consist of ONM nesprin and INM SUN proteins and have been implicated in microtubule-dependent, but not actin-dependent, nuclear movements (2, 11–13). Nevertheless, the largest splice forms of two mammalian nesprins, nesprin1 and nesprin2, contain cytoplasmically oriented paired actin-binding calponin homology (CH) domains (2).

To test whether nesprins were involved in nuclear movement, we initially expressed dominant negative constructs [red fluorescent protein-spectrin repeat-Klarsicht/ANC-1/Syne homology (RFP-SR-KASH) and RFP-KASH] of the LINC complex in wound-edge NIH3T3 fibroblasts and then stimulated nuclear movement with LPA. Expression of these constructs, known to disrupt LINC complexes and displace nesprins from the nuclear envelope (2, 3,

[4]To whom correspondence should be addressed. ggg1@columbia.edu.
[*]these authors contributed equally to this work

14), inhibited centrosome orientation and rearward nuclear positioning, while a control construct (RFP-KASHΔL) lacking the lumenal SUN-binding domain had no effect (Fig. 1A–C, and fig. S1). Live cell imaging showed that RFP-KASH blocked nuclear movement (Fig. 1D and movie S1). Thus, nesprins and the LINC complex are involved in centrosome orientation and nuclear movement. We cannot exclude the possibility that nesprins function in centrosome positioning, as nuclear movement is needed to observe centrosome centration defects (5, 15).

Expression analysis and immunoblotting showed that NIH3T3 fibroblasts express only one of the actin-binding, giant nesprin isoforms, nesprin2G (fig. S2A to C). Depletion of nesprin2G with siRNA blocked centrosome orientation due to defective rearward nuclear movement, whereas control siRNAs had no effect (Fig. 1E, figs. S2 to 4 and movies S2 and S3). These effects of nesprin2G-depletion were not due to gross alterations in the nuclear envelope because the levels and localization of five other nuclear envelope proteins were not greatly altered (fig. S4).

The centrosome and nuclear defects in nesprin2G-depleted cells were rescued by expression of GFP-mini-N2G, which contains the N-terminal CH domains and a C-terminal region containing spectrin repeats and the KASH domain of nesprin2G (Fig. 1E, fig S5 and S6). GFP-mini-N2G lacking the CH domains (ΔCH) or mutated to reduce F-actin-binding [Ile128→Ala128 and Ile131→Ala131 (abbreviated as I128, 131A in Fig. 1)] failed to rescue the polarity defects in nesprin2G-depleted cells (Fig.1E, figs. S5 and S6). Thus, nesprin2G and its actin-binding CH domains are necessary for nuclear movement.

We next asked whether moving nuclei associated with actin filaments. LPA stimulates actin filament formation in serum-starved cells (5, 16–18), and we found that an irregular actin meshwork formed near the nucleus at early times after LPA-stimulation (Fig. 2A). This meshwork rearranged by the time nuclear movement began (~30 min LPA stimulation) into distinct actin cables on the dorsal and ventral surfaces of the cell (Fig. 2A and B and fig. S7). The dorsal cables were usually parallel to the leading edge and resembled transverse actin arcs previously described in migrating cells (19, 20). The ventral cables were typically orthogonal to the leading edge and unlike the dorsal cables, terminated with focal adhesion markers and thus represent stress fibers (fig. S8) (18). The number of dorsal cables near nuclei increased during nuclear movement (30–90 min) (Fig. 2B and fig. S7).

Live imaging of actin filaments labeled with Lifeact-mCherry (21), which did not perturb actin, centrosome orientation or nuclear positioning (fig. S9), also showed dorsal and ventral actin cables near the nucleus (Fig. 2C and D). After LPA-stimulation, dorsal cables and the nucleus moved rearward at the same rate (0.35 +/− 0.10 μm/min) (Fig. 2C to E , and movie S4). Ventral stress fibers remained stationary or shortened slightly (Fig. 2C, fig. S10 and movie S5), suggesting that nuclear movement may be driven by the dorsal cables. Nesprin2G-depleted cells formed well-organized dorsal cables, which moved at the same rate (0.35 +/− 0.13 μm/min) as in control cells, yet nuclei in nesprin2G-depleted fibroblasts barely moved (0.06 +/− 0.09 μm/min) (Fig. 2D and E, and fig. S11). Thus, nesprin2G is not required for the organization or retrograde transport of dorsal cables.

In nesprin2G-depleted cells rescued with GFP-mini-N2G, linear structures that colocalized with dorsal cables were detected in the nuclear envelope (Fig. 3A). Endogenous nesprin2G was also observed in linear arrays that colocalized with dorsal cables in LPA-stimulated cells (Fig. 3A). This localization of GFP-miniN2G required functional CH domains (fig. S12) and actin cables, as actin or myosin II inhibitors prevented their formation (Fig. 3B). Fluorescence recovery after photobleaching revealed that the mobility of GFP-mini-N2G in the linear arrays was reduced compared to that in the bulk nuclear membrane (fig. S13).

SUN2 was the only other nuclear protein (among SUN1, SUN2, LBR, lamin A/C or lamin B1) that colocalized with linear arrays of GFP-mini-N2G (Fig. 3C and fig. S14). Expressed GFP-SUN2 also formed linear arrays on the dorsal surface of nuclei (fig. S15). Because the linear arrays are actin-depended, specific molecular assemblies of nesprin2G and SUN2 and not deformations of the nuclear envelope we refer to them as TAN (transmembrane actin-associated nuclear) lines.

SUN2 depletion also inhibited nuclear positioning and centrosome orientation (Fig. 3D and figs. S4 and S16). Unlike other nuclear envelope proteins examined, nesprin2G levels and nuclear localization were reduced by SUN2 depletion (fig. S4). Expressed GFP-SUN2, but not GFP-SUN1, rescued the polarity defects in SUN2-depleted cells. These results indicate that SUN1 and SUN2 are not functionally equivalent for nuclear movement (Fig. 3D and fig. S16). GFP-mini-N2G expression in SUN2-depleted cells failed to restore centrosome orientation and nuclear positioning further suggesting that nesprin2G requires SUN2 for normal nuclear movement (Fig. 3D and fig. S16).

During nuclear movement, GFP-mini-N2G TAN lines were observed moving rearward with the nucleus and dorsal actin cables labeled with Lifeact-mCherry (Fig. 4A to D, fig. S17, and movies S6 and S7). Velocity measurements confirmed this correlation for many moving nuclei (Fig. 4C). Dual imaging of GFP-TAN lines and Lifeact-mCherry additionally revealed that TAN lines formed after dorsal cables (Fig. 4D, arrows). Thus, actin organizes TAN lines, which may form to functionally harness the force of retrograde actin flow for nuclear movement.

Centrosome orientation has been implicated in directed cell migration (5, 15). We determined whether inhibition of centrosome orientation by disrupting nuclear movement affected cell migration. Nesprin2G- or SUN2-depleted cells migrated into in vitro wounds slower than control cells did, consistent with previous results (fig. S18, A and B) (12). Furthermore, wound-edge cells expressing RFP-KASH fell behind the wound-edge compared to cells expressing control constructs (fig. S19, C and D). Thus, the LINC complex and nuclear movement are required for efficient cell migration.

Here, the LINC complex components nesprin2G and SUN2 were found to assemble into TAN lines that provide a direct linkage between the nucleus and retrograde moving dorsal actin cables. Because each component of the TAN lines (nesprin2G, SUN2 and actin cables) was required for nuclear movement and TAN lines moved with dorsal cables during nuclear movement, we suggest that this assembly transmits force from retrograde actin flow to the nucleus. The accumulation of multiple nesprin2G and SUN2 molecules along an actin cable may be necessary to resist forces exerted by retrograde actin flow. Analogous force-resisting mechanisms were proposed for yeast KASH and SUN protein arrays, although these appear as spotwelds and anchor microtubules to the nuclear envelope (22).

We propose that TAN lines are functionally analogous to focal adhesions, which are clustered transmembrane integrins and associated cytoplasmic proteins that link the extracellular matrix to actin filaments. Both structures assemble in response to actin bundling by non-muscle myosin II and both transmit force across membranes. Unlike focal adhesions, TAN lines span two membranes and form along the length of an actin cable. Because INM SUN2 does not directly contact cytoplasmic dorsal actin cables, a regulatory “outside-in” signaling pathway, analogous to that for integrins (23), may exist allowing SUN2 to recognize nesprin2G engaged with actin and assembled into TAN lines. Recent work in mice suggests that nesprins and SUNs are important for normal mammalian development (13, 24, 25). It will be interesting to explore whether these proteins need to form a macromolecular structure like TAN lines to function during development.

Materials and Methods

See Supporting Materials

Supplementary Material

Refer to Web version on PubMed Central for supplementary material.

Acknowledgments

We thank W. Dauer, H. Herrmann, E. Marcantonio, G. Morris, S. Shackleton, R. Wedlich-Soldner, and H. Worman for providing reagents; members of the Dauer, Hirano, and Worman labs for helpful discussions; and Y. Zhao for analysis. This work was supported by a Dystonia Medical Research Foundation Fellowship (GWGL), an American Heart Association Fellowship (ESF), a Muscular Dystrophy Association grant (ERG), an Association pour la Recherche sur le Cancer grant (ERG), a Ligue Nacionale contre le Cancer grant (ERG), a Dystonia Medical Research Foundation grant (GGG) and NIH (GM06929; NS059352) grants (GGG).

References and Notes

1. Reinsch S, Gonczy P. J Cell Sci. 1998 Aug.111(Pt 16):2283. [PubMed: 9683624]
2. Starr DA. J Cell Sci. 2009 Mar 1.122:577. [PubMed: 19225124]
3. Wilhelmsen K, Ketema M, Truong H, Sonnenberg A. J Cell Sci. 2006 Dec 15.119:5021. [PubMed: 17158909]
4. Del Bene F, Wehman AM, Link BA, Baier H. Cell. 2008 Sep 19.134:1055. [PubMed: 18805097]
5. Gomes ER, Jani S, Gundersen GG. Cell. 2005 May 6.121:451. [PubMed: 15882626]
6. Goulding MB, Canman JC, Senning EN, Marcus AH, Bowerman B. J Cell Biol. 2007 Sep 24.178:1177. [PubMed: 17893243]
7. Ketelaar T, et al. Plant Cell. 2002 Nov.14:2941. [PubMed: 12417712]
8. Ramos-Garcia SL, Roberson RW, Freitag M, Bartnicki-Garcia S, Mourino-Perez RR. Eukaryot Cell. 2009 Dec.8:1880. [PubMed: 19684281]
9. Solecki DJ, et al. Neuron. 2009 Jul 16.63:63. [PubMed: 19607793]
10. Tsai JW, Bremner KH, Vallee RB. Nat Neurosci. 2007 Aug.10:970. [PubMed: 17618279]
11. Crisp M, et al. J Cell Biol. 2006 Jan 2.172:41. [PubMed: 16380439]
12. Luke Y, et al. J Cell Sci. 2008 Jun 1.121:1887. [PubMed: 18477613]
13. Zhang X, et al. Neuron. 2009 Oct 29.64:173. [PubMed: 19874786]
14. Starr DA, Han M. Science. 2002 Oct 11.298:406. [PubMed: 12169658]
15. Schmoranzer J, et al. Curr Biol. 2009 Jun 17.
16. Ridley AJ, Hall A. Cell. 1992 Aug 7.70:389. [PubMed: 1643657]
17. Ridley AJ, Paterson HF, Johnston CL, Diekmann D, Hall A. Cell. 1992 Aug 7.70:401. [PubMed: 1643658]
18. Naumanen P, Lappalainen P, Hotulainen P. J Microsc. 2008 Sep.231:446. [PubMed: 18755000]
19. Heath JP. Cell Biol Int Rep. 1981 Oct.5:975. [PubMed: 7197197]
20. Heath JP. J Cell Sci. 1983 Mar.60:331. [PubMed: 6348051]
21. Riedl J, et al. Nat Methods. 2008 Jul.5:605. [PubMed: 18536722]
22. King MC, Drivas TG, Blobel G. Cell. 2008 Aug 8.134:427. [PubMed: 18692466]
23. Legate KR, Wickstrom SA, Fassler R. Genes Dev. 2009 Feb 15.23:397. [PubMed: 19240129]
24. Lei K, et al. Proc Natl Acad Sci U S A. 2009 Jun 23.106:10207. [PubMed: 19509342]
25. Zhang X, et al. Development. 2007 Mar.134:901. [PubMed: 17267447]
26. Palazzo AF, et al. Curr Biol. 2001 Oct 2.11:1536. [PubMed: 11591323]

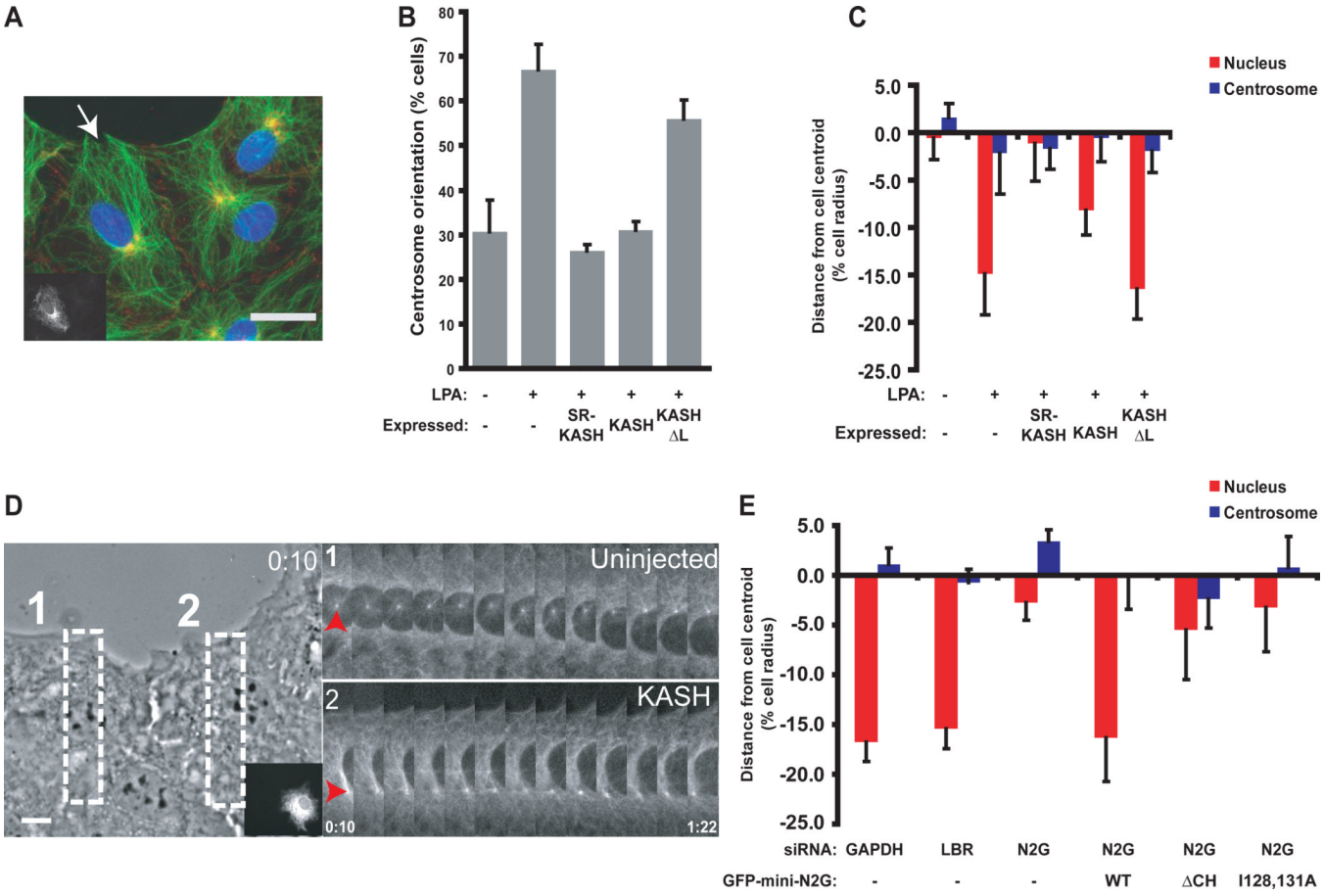

Fig. 1.

Nuclear movement requires nesprin2G. Wound edge is toward the top of all images. **A**, Representative wide-field epifluorescence image of centrosome orientation in RFP-KASH-expressing cells (cell expressing RFP-KASH is shown in insert and by arrow). Cells were stained as follows: DNA (blue), centrosomes (anti-pericentrin, yellow) and cell-cell contacts (anti-β-catenin, red). **B**, Centrosome orientation in cells expressing the indicated constructs. Random reorientation is ~33% (26). **C**, Average centrosome and nucleus positions along the axis perpendicular to the wound from cells described in **B**. The cell center is defined as "0". Positive values are toward the leading edge; negative values away. **D**, Nuclear movement in RFP-KASH-expressing (insert), GFP-α-tubulin NIH3T3 fibroblasts. (Left) Phase contrast image from the start of movie S1. Boxes indicate regions used for the GFP-α-tubulin fluorescence kymographs on the right. Arrowheads indicate centrosomes. Time is in hour:min. **E**, Average centrosome and nucleus positions from siRNA-treated cells expressing the indicated GFP-tagged constructs (N2G is nesprin2G). LBR is lamin B receptor; WT wild type; N2G nesprin2G. Experiments were repeated ≥ 3 times (N>30 for **B and C**; N>33 for **E)**. Error bars indicate SEM. Scale bars in **A,** 15 μm; **D,** 10 μm.

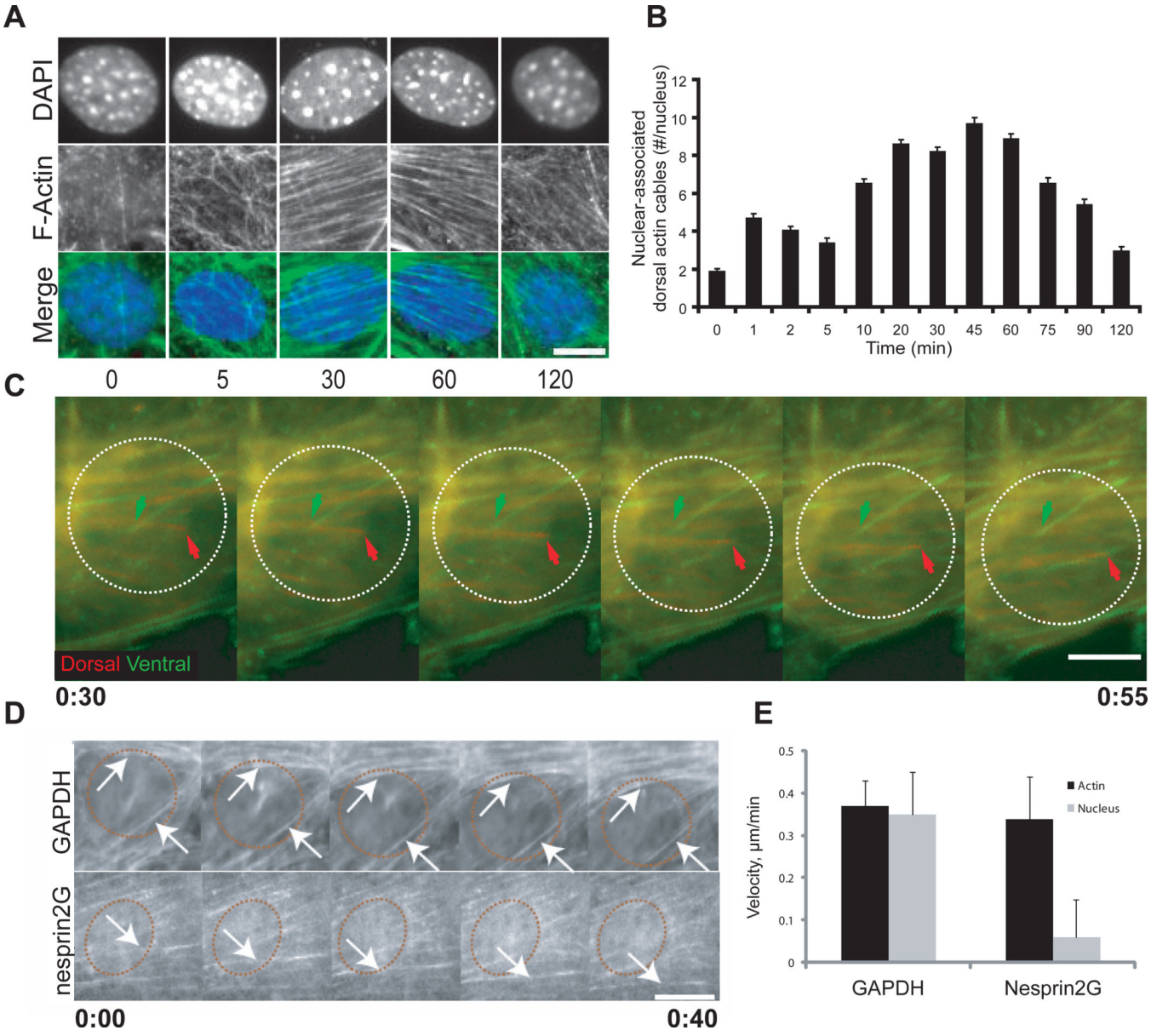

Fig. 2.

Coupled movement of dorsal actin cables and the nucleus. The wound edge is toward the top of all images. **A,** Representative wide-field epifluorescence images of nuclei in cells fixed after LPA-treatment. Time is in min. Cells were stained as follows: DNA [4′,6′-diamidino-2-phenylindole (DAPI)] and F-actin (rhodamine-phalloidin). **B,** Number of dorsal cables spanning the entire nucleus from cells treated as in **A**. Experiments were repeated 3 times with N > 151. **C**, Fluorescence kymograph of a Lifeact-mCherry-expressing cell from movie S4 and S5. Fluorescence images were acquired from dorsal and ventral planes of the cell, pseudocolored and merged. Nuclear position, dashed white circle. Arrows indicate dorsal (red) and ventral (green) cables. Images taken every 5 min. **D**, Fluorescence kymographs of Lifeact-mCherry in GAPDH- or nesprin2G-depleted cells. Nuclear position, red dashed circle. Images are every 10 min. Arrows indicate moving dorsal actin cables. **E**, LPA-stimulated dorsal cable and nucleus velocities in cells treated as in **D**. Data are from 5

independent experiments (N=36 (GAPDH) and 27 (nesprin2G)). Error bars indicate SEM. Scale bars for **A** and **C,** 5 μm; **D,** 10 μm.

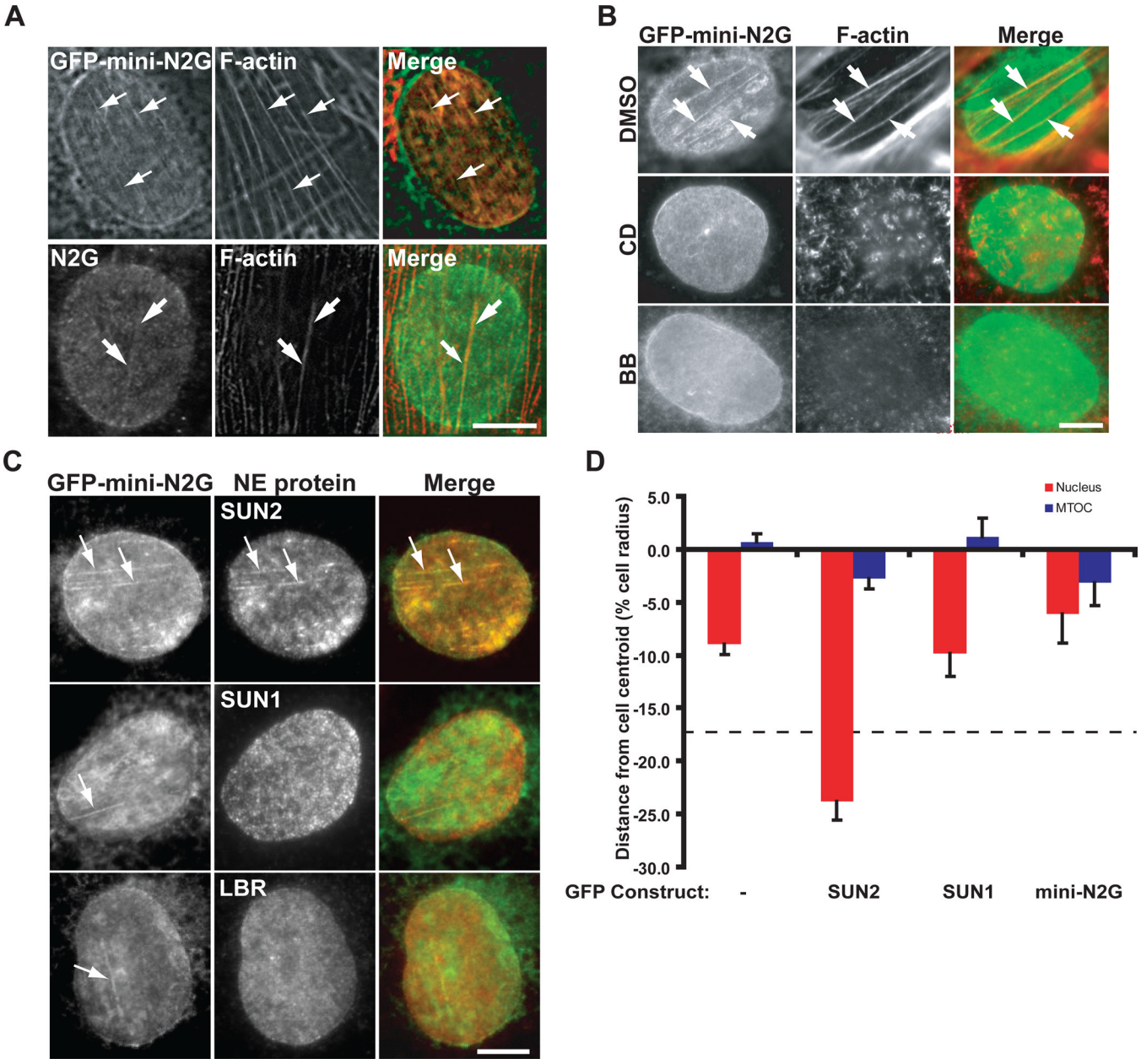

Fig. 3.

Nesprin2G and SUN2 form TAN lines. All images are of the dorsal nuclear surface. **A**, Top) Fluorescence images of a nucleus from a nesprin2G-depleted cell expressing GFP-mini-N2G and stained with rhodamine-phalloidin (F-actin). (Bottom) Fluorescent images of a nucleus in a cell stained with nesprin2G antibody (N2G) and rhodamine-phalloidin (F-actin). Arrows, colocalized N2G and dorsal actin cables. Wound edges are toward the upper right (top) and right (bottom). **B**, Fluorescence images of nuclei in nesprin2G-depleted cells expressing GFP-mini-N2G. Cells were stained with GFP antibody (GFP-mini-N2G) and rhodamine-phalloidin (F-actin). Cells were treated with dimethyl sulfoxide (DMSO), 50 μM blebbistatin (BB) or 0.5 μM cytochalasin D (CD) for 1 hr before and during LPA treatment. The wound-edge is toward the top left. **C**, Fluorescence images of nuclei in nesprin2G-depeleted cells. Cells were stained with SUN1, SUN2, LBR and GFP (GFP-mini-N2G)

antibodies. Arrows show N2G colocalizing with SUN2, but not SUN1 or LBR. The wound-edge is toward the top. **D**, Average centrosome and nucleus positions from SUN2-depleted cells expressing the indicated GFP-tagged constructs. Dashed line represents average nuclear position in non-depleted cells. Experiments were repeated ≥ 3 times with N>201. Error bars, SEM. Bars in **A** to **C**, 5 μm.

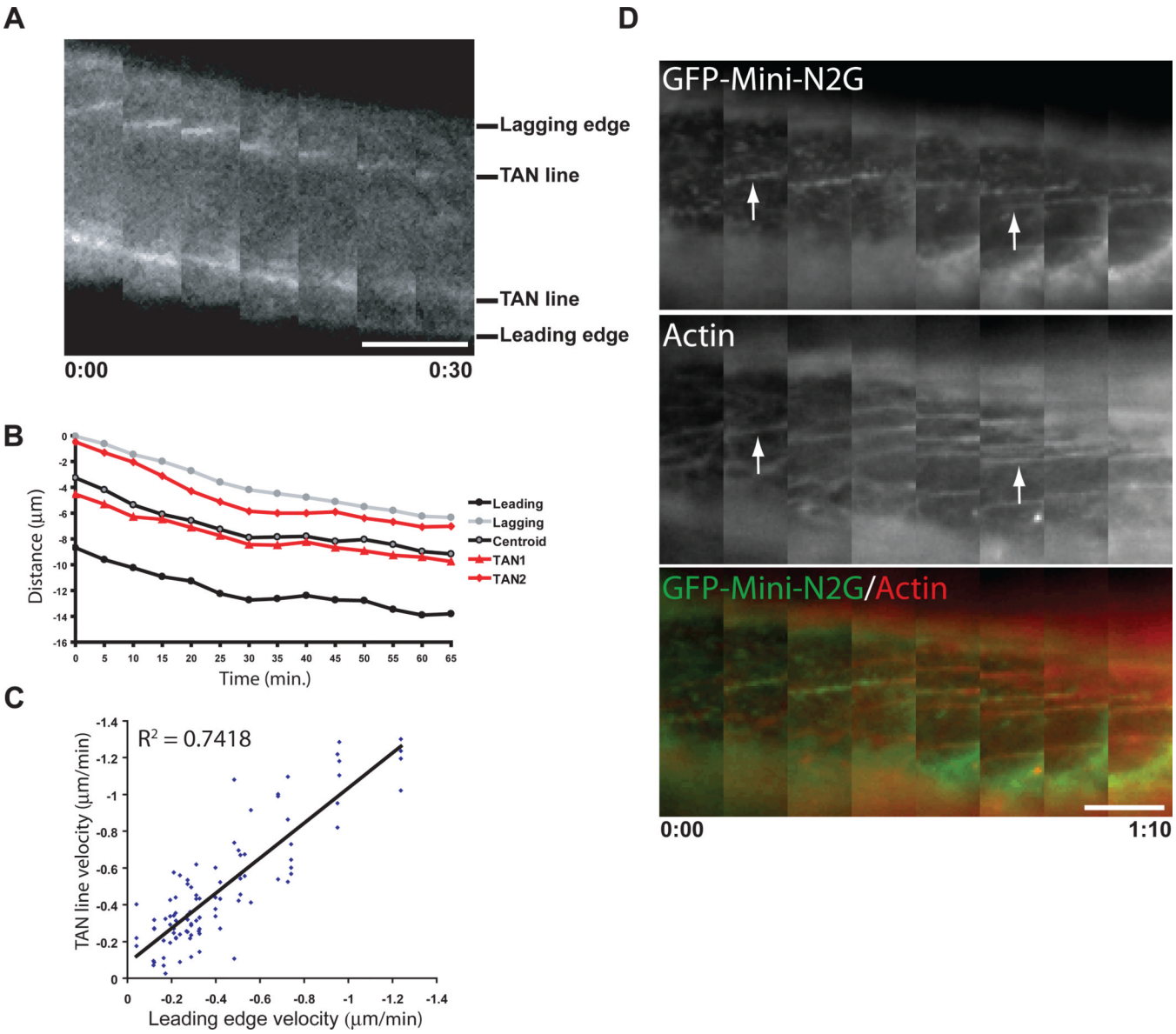

Fig. 4.

TAN lines are coupled with dorsal actin cables during nuclear movement. **A**, Fluorescence kymograph of GFP-mini-N2G TAN lines in a nucleus from a nesprin2-depleted cell from movie 6. The leading and lagging edges of the nucleus and two TAN lines are indicated. Each image is 5 min. **B**, Representative distance versus time plot of TAN lines, nuclear centroid, and leading and lagging nuclear edges from a movie of a cell treated as in **A**. **C**, Comparison of GFP-mini-N2G TAN line and leading nuclear edge velocities in cells treated as in **A**. Data are from 30 movies of 30 cells. R^2 is the coefficient of determination. **D**, Fluorescence kymograph of GFP-miniN2G and Lifeact-mCherry on the dorsal nuclear surface of a nucleus in a cell treated as in **A** from movie 7. Arrows indicate examples of TAN lines forming on actin cables. Panels are every 10 min and oriented with the wound-edge at the top. Time is hour:min for **A** and **D**. Scale bars in **A** and **D,** 5 μm.